

General Disclaimer

One or more of the Following Statements may affect this Document

- This document has been reproduced from the best copy furnished by the organizational source. It is being released in the interest of making available as much information as possible.
- This document may contain data, which exceeds the sheet parameters. It was furnished in this condition by the organizational source and is the best copy available.
- This document may contain tone-on-tone or color graphs, charts and/or pictures, which have been reproduced in black and white.
- This document is paginated as submitted by the original source.
- Portions of this document are not fully legible due to the historical nature of some of the material. However, it is the best reproduction available from the original submission.

50 Copies

NATIONAL AERONAUTICS AND SPACE ADMINISTRATION

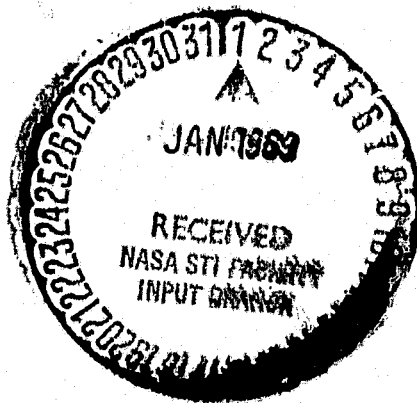
Technical Report 32-1333

**Multipath, Polarization, and Pointing Losses
From a Mars Lander**

H. K. Frewing

FACILITY FORM 602

N 69-13928 (ACCESSION NUMBER)	_____ (THRU)
29 (PAGES)	1 (CODE)
CR-98570 (NASA CR OR TMX OR AD NUMBER)	07 (CATEGORY)



**JET PROPULSION LABORATORY
CALIFORNIA INSTITUTE OF TECHNOLOGY
PASADENA, CALIFORNIA**

December 15, 1968

NATIONAL AERONAUTICS AND SPACE ADMINISTRATION

Technical Report 32-1333

*Multipath, Polarization, and Pointing Losses
From a Mars Lander*

H. K. Frewing

JET PROPULSION LABORATORY
CALIFORNIA INSTITUTE OF TECHNOLOGY
PASADENA, CALIFORNIA

December 15, 1968

TECHNICAL REPORT 32-1333

Copyright © 1968

**Jet Propulsion Laboratory
California Institute of Technology**

**Prepared Under Contract No. NAS 7-100
National Aeronautics & Space Administration**

Preface

The work described in this report was performed by the Project Engineering Division of the Jet Propulsion Laboratory.

Acknowledgment

Lowell Howard has been of invaluable help in deriving the antenna gain approximation and in doing the computer programming required for this simulation.

E. C. de Wys developed the Mars surface models.

Kane Casani suggested this approach for estimating Mars lander communication system losses.

Dean Boyd carried out the initial electromagnetic analysis for estimating multipath degradation from a Mars lander.

Floyd Jean, Richard Dickinson and John Gerpheide have critically reviewed the manuscript and have made valuable revision suggestions.

Contents

I. Introduction	1
II. Loss Equations	2
A. Pointing Loss	2
B. Multipath Loss	2
C. Polarization Loss	6
III. Coordinate Transformations	9
A. Mars-Centered Coordinate System	9
B. Landing-Site-Centered Coordinate System	10
C. Lander-Centered Coordinate System	10
IV. Loss Results	11
V. Conclusions	12
Reference	13
Appendix A. Computation of Fresnel Zones	14
Appendix B. Random Variable Distributions and Antenna Characteristics	15
Appendix C. Losses as a Function of Mars Rotation	17
Appendix D. Computer Program for Loss Computation	18

Table

1. Antenna configuration	12
--------------------------	----

Figures

1. JPL CSAD lander antenna configuration	1
2. Lander transmitter geometry	2
3. CSAD lander radio electric field vector phase diagram	8
4. Mars-centered coordinate system	9

Contents (contd)

Figures (contd)

5. Landing-site-centered coordinate system	10
6. Lander-centered coordinate system	10
7. Pointing, multipath, polarization, and combined loss distributions for circular polarization at landing	13
8. Pointing, multipath, polarization, and combined loss distributions for circular polarization 21.3 h after landing	13
A-1. Rayleigh criterion for specular reflection at S-band (13 cm)	14
A-2. Fresnel zone calculation geometry	14
B-1. Probability density functions of Martian slopes	15
B-2. Antenna gain characteristics	16
C-1. Multipath and pointing losses vs planet rotation	17

Abstract

A model and a computer simulation program have been developed for statistically estimating the multipath, polarization, and pointing losses associated with the communication link from a planetary lander. The model allows these losses to be estimated for a lander of any configuration, with any antenna array, with any antenna characteristics and impacting at any position on any planet. It accounts for the random distribution of surface slopes likely to be encountered by a planetary lander. It assumes specular reflection of circular polarized waves as the multipath interference mechanism.

Equations for computing multipath, polarization, and pointing losses are derived, as are the coordinate transformations required for converting the random impact conditions of a planetary lander into quantities required for the electromagnetic equations. One hundred computer-simulated landings of a Jet Propulsion Laboratory (JPL) Mars rough lander are carried out for one landing in which the earth is 45 deg above the western horizon and for another landing in which the earth is overhead. Statistical distributions of combined multipath, polarization, and pointing losses are computed for each of these landing conditions.

Appendixes justify the use of the planet surface model assumed, provide estimates of the surface slope distribution of the planet and of the antenna characteristics of the lander, compute combined losses as a function of planet rotation, and include a copy of the computer listing for the particular example given.

Multipath, Polarization, and Pointing Losses From a Mars Lander

I. Introduction

A performance estimate of a planetary lander communication link to earth requires knowledge of multipath, polarization, and pointing losses. A statistical method of estimating these losses from planetary landers has been developed. The technique is generally applicable to a wide variety of planetary lander antenna configurations and communication link geometries. The technique requires only a knowledge of (1) the lander antenna geometry and gain patterns, (2) the lander impact position, (3) the location of the sub-earth point, (4) the probability density of the planetary surface slopes, and (5) the physical characteristics of the planet's surface. This information is then used to derive the expected losses and to place tolerances on these expected losses. The losses derived from this technique are from 5-10 dB less than those that would be obtained if the worst multipath, polarization, and pointing losses were assumed.

To estimate these losses, a series of computer-simulated landings¹ have been carried out using the Jet Propulsion Laboratory (JPL) Capsule System Advanced Development (CSAD) project Mars lander. This disc-shaped lander provides omnidirectional antenna coverage by

¹Mars '71 Technical Study, JPL internal document, Edited by E. K. Casani, JPL, Aug. 15, 1966.

²A Possible 1971 Mariner Mars Landed Experiment, JPL Flight Projects document, July 24, 1967.

having six right-hand circularly polarized antennas positioned with their boresights perpendicular to the faces of a cube. Two antennas point horizontally in the plane of the lander, and four antennas point at 45 deg to the plane of the lander disc. A geometrical schematic of this lander is shown in Fig. 1. The lander contains an S-band transmitter.

At each simulated impact, the lander hits the Martian surface at about noon with the earth about 45 deg above the western horizon. It lands on a randomly generated slope that is determined by using an estimated slope

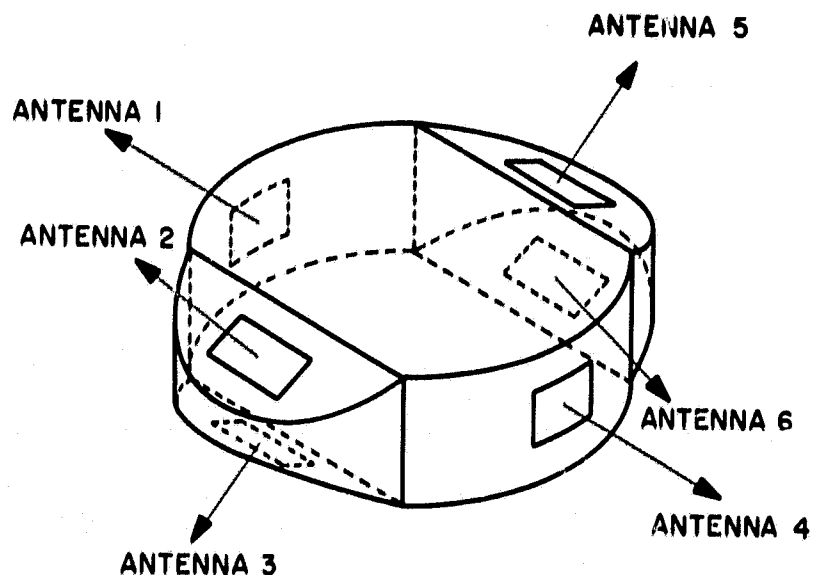


Fig. 1. JPL CSAD lander antenna configuration

probability density function. The orientation of this slope is also randomly generated. The plane of the lander disc is assumed to be parallel to the slope, but the lander assumes a random azimuth angle with respect to the maximum gradient of the slope.

Multipath, polarization, and pointing losses are then calculated for all six antennas at each landing. The following morning, about 21.3 h after landing, the losses are calculated again when the earth is almost directly above the lander.

Section II derives the electromagnetic equations for computing multipath, polarization, and pointing losses of a right-hand circularly polarized wave. Section III derives the coordinate transformations required for obtaining angular quantities in lander-centered coordinates as functions of angles in Mars-centered and landing-site-centered coordinates.

Appendix A justifies the use of the planet surface model by showing that the physical parameters assumed are likely to hold over the first Fresnel zone. Appendix B gives the random variable distributions and the antenna characteristics assumed. The combined losses are computed as a function of planet rotation in Appendix C. A sample computer program listing for computing the losses of 100 random landings is given in Appendix D.

II. Loss Equations

A. Pointing Loss

The pointing loss of a particular antenna is defined as the ratio of the radiated power in the direction of the receiver to the power at the peak of the antenna pattern. Symbolically,

$$L_{point} = \frac{G^2(\zeta_d)}{G^2(0)}$$

where L_{point} is a dimensionless ratio, $G(\zeta_d)$ is the antenna field strength gain with respect to an isotropic antenna in the direction of the receiver, and $G(0)$ is the antenna field strength gain at the peak of the pattern with respect to an isotropic antenna. $G(\zeta_d)$ and $G(0)$ are dimensionless quantities—not expressed in dB. The angle ζ_d is the cone angle in the direction of the receiver measured from the peak of the pattern. Pointing loss, expressed in dB is:

$$L_{point} (dB) = 10 \log_{10} L_{point} = 10 \log_{10} \frac{G^2(\zeta_d)}{G^2(0)}$$

B. Multipath Loss

Multipath loss for the circularly polarized wave considered here is defined as the ratio of the power in the combined direct and reflected wave to the power in the direct wave. If the reflected wave constructively interferes with the direct wave, there is no multipath loss; there is multipath gain instead. Conversely, if the reflected wave destructively interferes with the direct wave, the radiated field strength is effectively reduced. The power ratio is then converted to dB. The geometry for defining multipath loss is shown in Fig. 2.

Before it is reflected from the planet's surface, a right-hand-circularly-polarized wave can be represented by an electric field vector given by

$$\mathbf{E}_r = G(\zeta_r) [\mathbf{e}_h \exp j(\omega t - kz) + \mathbf{e}_v \exp j(\omega t - kz - \pi/2)]$$

where

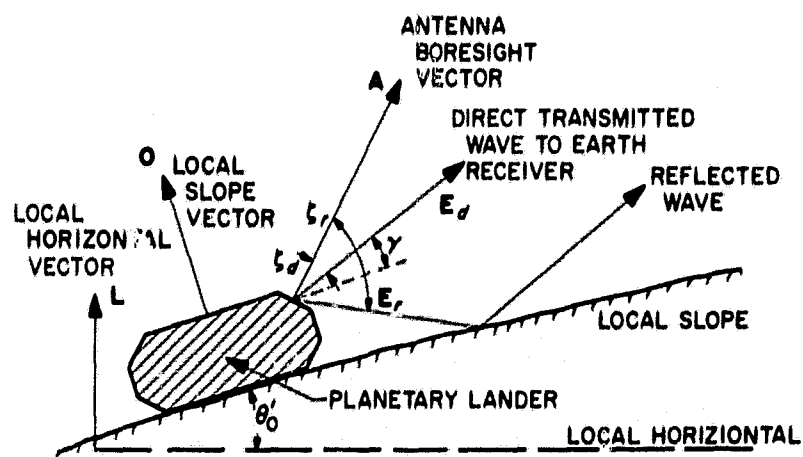
ζ_r = reflected wave cone angle measured from pattern maximum

$G(\zeta_r)$ = antenna field strength gain in direction of reflected wave before reflection (with respect to isotropic antenna field strength)

\mathbf{e}_h = unit vector in horizontal polarization direction

\mathbf{e}_v = unit vector in vertical polarization direction

and where $\exp j(\omega t - kz)$ and $\exp j(\omega t - kz - \pi/2)$ are the complex representations of field strength phase as a function of time and distance along the propagation path.



NOTE: VECTORS ARE NOT ALWAYS COPLANAR AS SHOWN

Fig. 2. Lander transmitter geometry

For a non-dissipative planetary atmosphere with the dielectric constant of free space, the propagation constant k is: $k = \omega (\mu_0 \epsilon_0)^{1/2}$.

After reflection from the planet's surface toward an earth receiver, the wave can be represented by the electric field vector:

$$\mathbf{E}'_r = G(\zeta_r) \rho_s D [\mathbf{e}'_h R_h \exp j(\omega t - kz + 2\pi\delta/\lambda + \phi_h) + \mathbf{e}'_v R_v \exp j(\omega t - kz - \pi/2 + 2\pi\delta/\lambda + \phi_v)]$$

where

\mathbf{e}'_h = unit vector in horizontal polarization direction after reflection

\mathbf{e}'_v = unit vector in vertical polarization direction after reflection

The factor $\exp(j2\pi\delta/\lambda)$ that occurs in both the vertical and horizontal reflected components represents the phase difference between the direct and reflected waves caused by the path length difference. In this expression,

δ = path difference between direct and reflected waves

λ = transmitted wave length

The path difference between the two waves is defined as:

$$\delta = \frac{h}{\sin \gamma} (1 - \cos 2\gamma)$$

where

h = antenna height above ground

γ = elevation angle of receiver above local slope measured in plane perpendicular to local slope

The factors D and ρ_s account for the wave reflection from a rough, curved, planet surface and are defined as:

ρ_s = coefficient accounting for the planet's roughness

D = coefficient accounting for dispersion due to curvature

For our case, D will be taken as unity since the transmitter is so close to the planet that the effect of its curvature is negligible. The roughness coefficient, ρ_s , will be assumed to be the rms value of ρ_s , although the surface roughness and therefore the surface roughness coefficient

are actually variables with statistical distributions; therefore

$$\rho_s = \exp \left[-\frac{1}{2} \left(\frac{4\pi\Delta h \sin \gamma}{\lambda} \right)^2 \right]$$

where Δh is the rms surface roughness height.

The factors $R_h \exp j\phi_h$ and $R_v \exp j\phi_v$ are the reflection coefficients from smooth, plane surfaces for horizontal and vertical polarization, respectively. In terms of the electrical parameters of the reflecting surface, these coefficients are

$$R_h \exp j\phi_h = \frac{\sin \gamma - (Y^2 - \cos^2 \gamma)^{1/2}}{\sin \gamma + (Y^2 - \cos^2 \gamma)^{1/2}}$$

and

$$R_v \exp j\phi_v = \frac{Y^2 \sin \gamma - (Y^2 - \cos^2 \gamma)^{1/2}}{Y^2 \sin \gamma + (Y^2 - \cos^2 \gamma)^{1/2}}$$

where Y is the planet's normalized admittance. The admittance is defined as

$$Y^2 = \frac{\epsilon/\epsilon_0 - j60\lambda\sigma}{\mu/\mu_0}$$

where

ϵ/ϵ_0 = ratio of permittivity of planet surface to permittivity of free space

μ/μ_0 = ratio of permeability of planet surface to permeability of free space

σ = conductivity of planet surface

These expressions for electromagnetic wave reflection from a rough planet surface are developed for other cases in Ref. 1.³ More basic derivations of electromagnetic and probability equations can be found in the citations given in Ref. 1.

The wave going directly from the antenna to the earth receiver can be represented by:

$$\mathbf{E}'_d = G(\zeta_d) [\mathbf{e}'_h \exp j(\omega t - kz) + \mathbf{e}'_v \exp j(\omega t - kz - \pi/2)]$$

³Also in *Estimation of Multipath Degradation for a Planetary Lander*, by D. Boyd, JPL Section Memorandum, September 13, 1967.

If the impedance of the planetary atmosphere is given by

$$\eta = \left(\frac{\mu_0}{\epsilon_0} \right)^{1/2} = - \frac{E_v}{E_h} = \frac{E_h}{H_v}$$

where E_v and E_h are any vertically and horizontally polarized electric-field vectors and H_v and H_h are appropriate vertically and horizontally polarized magnetic-field

vectors, the magnetic field of the wave traveling directly to earth is given by

$$\mathbf{H}'_d = \frac{G(\zeta_d)}{\eta} [-\mathbf{e}'_h \exp j(\omega t - kz - \pi/2) + \mathbf{e}'_v \exp j(\omega t - kz)]$$

The complex conjugate of the direct wave's magnetic field is then:

$$\mathbf{H}'_d^* = \frac{G(\zeta_d)}{\eta} [-\mathbf{e}'_h \exp -j(\omega t - kz - \pi/2) + \mathbf{e}'_v \exp -j(\omega t - kz)]$$

The total wave traveling toward the earth receiver is the sum of the direct and reflected waves. This wave can be represented by:

$$\begin{aligned} \mathbf{E}'_t &= \mathbf{E}'_d + \mathbf{E}'_r = \mathbf{e}'_h [G(\zeta_d) \exp j(\omega t - kz) + \rho_s DR_h G(\zeta_r) \exp j(\omega t - kz + 2\pi\delta/\lambda + \phi_h)] \\ &\quad + \mathbf{e}'_v [G(\zeta_d) \exp j(\omega t - kz - \pi/2) + \rho_s DR_v G(\zeta_r) \exp j(\omega t - kz - \pi/2 + 2\pi\delta/\lambda + \phi_v)] \\ &= \mathbf{e}'_h \exp j(\omega t - kz) [G(\zeta_d) + \rho_s DR_h G(\zeta_r) \exp j(2\pi\delta/\lambda + \phi_h)] \\ &\quad + \mathbf{e}'_v \exp j(\omega t - kz - \pi/2) [G(\zeta_d) + \rho_s DR_v G(\zeta_r) \exp j(2\pi\delta/\lambda + \phi_v)] \end{aligned}$$

The total magnetic field in the direction of the earth receiver is

$$\begin{aligned} \mathbf{H}'_t &= - \frac{\mathbf{e}'_h}{\eta} \exp j(\omega t - kz - \pi/2) [G(\zeta_d) + \rho_s DR_v G(\zeta_r) \exp j(2\pi\delta/\lambda + \phi_v)] \\ &\quad + \frac{\mathbf{e}'_v}{\eta} \exp j(\omega t - kz) [G(\zeta_d) + \rho_s DR_h G(\zeta_r) \exp j(2\pi\delta/\lambda + \phi_h)] \end{aligned}$$

The complex conjugate of this magnetic field vector is

$$\begin{aligned} \mathbf{H}'_t^* &= - \frac{\mathbf{e}'_h}{\eta} \exp -j(\omega t - kz - \pi/2) [G(\zeta_d) + \rho_s DR_v G(\zeta_r) \exp -j(2\pi\delta/\lambda + \phi_v)] \\ &\quad + \frac{\mathbf{e}'_v}{\eta} \exp -j(\omega t - kz) [G(\zeta_d) + \rho_s DR_h G(\zeta_r) \exp -j(2\pi\delta/\lambda + \phi_h)] \end{aligned}$$

The average power in an electromagnetic wave is the average value of the Poynting vector which is given by

$$\mathbf{S} = \frac{1}{2} \text{Re} [\mathbf{E} \times \mathbf{H}^*] = \frac{1}{2} \text{Re} [-E_v H_h^* + E_h H_v^*]$$

where \mathbf{E} and \mathbf{H} are the electric and magnetic-field components of any electromagnetic wave, and E_v , H_v , E_h and H_h are the vertically and horizontally polarized components of an electromagnetic wave that can be represented by vertically and horizontally polarized components.

In the case of the wave traveling directly to earth, the average power is:

$$\begin{aligned}
 S'_d &= \frac{1}{2} \operatorname{Re} \left\{ - (-) G(\zeta_d) \exp j(\omega t - kz - \pi/2) \frac{G(\zeta_d)}{\eta} \exp - j(\omega t - kz - \pi/2) \right. \\
 &\quad \left. + G(\zeta_d) \exp j(\omega t - kz) \frac{G(\zeta_d)}{\eta} \exp - j(\omega t - kz) \right\} \\
 &= \frac{1}{2} \operatorname{Re} \left\{ \frac{G^2(\zeta_d)}{\eta} + \frac{G^2(\zeta_d)}{\eta} \right\} \\
 &= \frac{G^2(\zeta_d)}{\eta}
 \end{aligned}$$

For the total wave directed toward the receiver, the average power is:

$$\begin{aligned}
 S'_t &= \frac{1}{2} \operatorname{Re} \left\{ \frac{1}{\eta} [G^2(\zeta_d) + \rho_s DR_v G(\zeta_d) G(\zeta_r) \exp j(2\pi\delta/\lambda + \phi_v) \right. \\
 &\quad \left. + \rho_s DR_v G(\zeta_d) G(\zeta_r) \exp - j(2\pi\delta/\lambda + \phi_v) + \rho_s^2 D^2 R_v^2 G^2(\zeta_r)] \right. \\
 &\quad \left. + \frac{1}{\eta} [G^2(\zeta_d) + \rho_s DR_h G(\zeta_d) G(\zeta_r) \exp j(2\pi\delta/\lambda + \phi_h) \right. \\
 &\quad \left. + \rho_s DR_h G(\zeta_d) G(\zeta_r) \exp - j(2\pi\delta/\lambda + \phi_h) + \rho_s^2 D^2 R_h^2 G^2(\zeta_r)] \right\} \\
 &= \frac{1}{2\eta} \left\{ [G^2(\zeta_d) + 2\rho_s DR_v G(\zeta_d) G(\zeta_r) \cos(2\pi\delta/\lambda + \phi_v) + \rho_s^2 D^2 R_v^2 G^2(\zeta_r)] \right. \\
 &\quad \left. + [G^2(\zeta_d) + 2\rho_s DR_h G(\zeta_d) G(\zeta_r) \cos(2\pi\delta/\lambda + \phi_h) + \rho_s^2 D^2 R_h^2 G^2(\zeta_r)] \right\}
 \end{aligned}$$

Multipath loss (or gain) is defined as the ratio of the average power in the total wave to the average power in the direct wave. This quotient yields circular polarization multipath loss as:

$$\begin{aligned}
 L_{multi} &= \frac{S'_t}{S'_d} = \frac{1}{2} \left\{ \left[1 + 2\rho_s DR_v \frac{G(\zeta_r)}{G(\zeta_d)} \cos(2\pi\delta/\lambda + \phi_v) + \rho_s^2 D^2 R_v^2 \frac{G^2(\zeta_r)}{G^2(\zeta_d)} \right] \right. \\
 &\quad \left. + \left[1 + 2\rho_s DR_h \frac{G(\zeta_r)}{G(\zeta_d)} \cos(2\pi\delta/\lambda + \phi_h) + \rho_s^2 D^2 R_h^2 \frac{G^2(\zeta_r)}{G^2(\zeta_d)} \right] \right\}
 \end{aligned}$$

But it can be shown that for a vertically polarized wave, multipath loss is:

$$L_{multi}^+ = 1 + 2\rho_s DR_v \frac{G(\zeta_r)}{G(\zeta_d)} \cos(2\pi\delta/\lambda + \phi_v) + \rho_s^2 D^2 R_v^2 \frac{G^2(\zeta_r)}{G^2(\zeta_d)}$$

and that multipath loss for a horizontally polarized wave is:

$$L_{multi}^- = 1 + 2\rho_s DR_h \frac{G(\zeta_r)}{G(\zeta_d)} \cos(2\pi\delta/\lambda + \phi_h) + \rho_s^2 D^2 R_h^2 \frac{G^2(\zeta_r)}{G^2(\zeta_d)}$$

Multipath loss for a circularly polarized wave is thus seen to be the average of vertically and horizontally polarized wave multipath losses, or:

$$L_{\text{multipath}} = 1/2(L_{\text{multipath}}^+ + L_{\text{multipath}}^-)$$

Multipath loss can be converted to dB by

$$L_{\text{multipath}}(\text{dB}) = 10 \log_{10} L_{\text{multipath}}$$

C. Polarization Loss

Polarization loss will be defined as the ratio of right-hand circularly polarized power to total power transmitted to earth. The total power includes the sum of power transmitted directly to earth plus the power reflected from the planet's surface due to multipath effects.

The electric vector of the total transmitted wave has been given as

$$\begin{aligned} \mathbf{E}_t = & \mathbf{e}_h G(\zeta_d) \exp j(\omega t - kz) \left[1 + \rho_n DR_h \frac{G(\zeta_r)}{G(\zeta_d)} \exp j(2\pi\delta/\lambda + \phi_h) \right] \\ & + \mathbf{e}_v G(\zeta_d) \exp j(\omega t - kz - \pi/2) \left[1 + \rho_n DR_v \frac{G(\zeta_r)}{G(\zeta_d)} \exp j(2\pi\delta/\lambda + \phi_v) \right] \end{aligned}$$

It is now desired to break up this total vector into right-hand and left-hand circularly polarized components. In general, the total wave is some sort of elliptically polarized wave, but the receiver will accept only the right-hand circularly polarized component. It is desired to put the total wave into the form

$$\begin{aligned} \mathbf{E}_t = & \mathbf{e}_h E_r \exp j(\omega t - kz) + \mathbf{e}_v E_r \exp j(\omega t - kz - \pi/2) \\ & + \mathbf{e}_h E_l \exp j(\omega t - kz) + \mathbf{e}_v E_l \exp j(\omega t - kz + \pi/2) \end{aligned}$$

where E_r and E_l must be related to the parameters of the total wave. To simplify the analysis, the total wave will be written in the form

$$\mathbf{E}_t = \mathbf{e}_h G(\zeta_d) \exp j(\omega t - kz) [1 + A_1 \exp j\theta_1] + \mathbf{e}_v G(\zeta_d) \exp j(\omega t - kz - \pi/2) [1 + A_2 \exp j\theta_2]$$

where

$$A_1 = \rho_n DR_h \frac{G(\zeta_r)}{G(\zeta_d)}$$

$$A_2 = \rho_n DR_v \frac{G(\zeta_r)}{G(\zeta_d)}$$

$$\theta_1 = 2\pi\delta/\lambda + \phi_h$$

$$\theta_2 = 2\pi\delta/\lambda + \phi_v$$

This form of the total wave vector can be further simplified to

$$\mathbf{E}_t = \mathbf{e}_h A_3 G(\zeta_d) \exp j(\omega t - kz + \theta_3) + \mathbf{e}_v A_4 G(\zeta_d) \exp j(\omega t - kz - \pi/2 + \theta_4)$$

where

$$A_3 = [(1 + A_1 \cos \theta_1)^2 + A_1^2 \sin^2 \theta_1]^{1/2}$$

$$A_4 = [(1 + A_2 \cos \theta_2)^2 + A_2^2 \sin^2 \theta_2]^{1/2}$$

$$\theta_3 = \arctan \left[\frac{A_1 \sin \theta_1}{1 + A_1 \cos \theta_1} \right]$$

$$\theta_4 = \arctan \left[\frac{A_2 \sin \theta_2}{1 + A_2 \cos \theta_2} \right]$$

The total wave expressed as the sum of right- and left-hand circularly polarized waves can be written as

$$\mathbf{E}_t = \mathbf{e}_h (E_r + E_l) \exp j(\omega t - kz) + \mathbf{e}_v \exp j(\omega t - kz) (E_r \exp -j\pi/2 + E_l \exp j\pi/2)$$

Equating the horizontal and vertical components to their respective expressions derived above requires that $E_r + E_l = A_3 G(\zeta_d) \exp j\theta_3$ and

$$-jE_r + jE_l = A_4 G(\zeta_d) \exp j(\theta_4 - \pi/2)$$

Solving these two simultaneous equations for E_r yields

$$\begin{aligned} E_r &= \frac{G(\zeta_d)}{2} [A_3 \cos \theta_3 - A_4 \sin(\theta_4 - \pi/2) + jA_3 \sin \theta_3 + jA_4 \cos(\theta_4 - \pi/2)] \\ &= A_5 \exp j\theta_5 \end{aligned}$$

where

$$A_5 = \frac{G(\zeta_d)}{2} \{ [A_3 \cos \theta_3 - A_4 \sin(\theta_4 - \pi/2)]^2 + [A_3 \sin \theta_3 + A_4 \cos(\theta_4 - \pi/2)]^2 \}^{1/2}$$

and where

$$\theta_5 = \arctan \left[\frac{A_3 \sin \theta_3 + A_4 \cos(\theta_4 - \pi/2)}{A_3 \cos \theta_3 - A_4 \sin(\theta_4 - \pi/2)} \right]$$

The electric field vector of the right-hand circular polarized component of the total wave then becomes

$$\mathbf{E}_r = \mathbf{e}_h A_5 \exp j(\omega t - kz + \theta_5) + \mathbf{e}_v A_5 \exp j(\omega t - kz - \pi/2 + \theta_5)$$

The magnetic field vector can be written

$$\mathbf{H}_r = -\mathbf{e}_h \frac{A_5}{\eta} \exp j(\omega t - kz - \pi/2 + \theta_5) + \mathbf{e}_v \frac{A_5}{\eta} \exp j(\omega t - kz + \theta_5)$$

and the complex conjugate of the magnetic field vector can be written

$$\mathbf{H}_r^* = -\mathbf{e}_h \frac{A_5}{\eta} \exp -j(\omega t - kz - \pi/2 + \theta_5) + \mathbf{e}_v \frac{A_5}{\eta} \exp -j(\omega t - kz + \theta_5)$$

The total power transmitted in the right-hand circular polarized component is then

$$\begin{aligned} S_r &= \frac{1}{2} \text{Re} \{ \mathbf{E}_r \times \mathbf{H}_r^* \} = \frac{1}{2} \text{Re} \{ A_5^2/\eta + A_5^2/\eta \} = A_5^2/\eta \\ &= \frac{G^2(\zeta_d)}{4\eta} [A_3^2 + A_4^2 + 2A_3 A_4 \cos(\theta_3 - \theta_4)] \\ &= \frac{G^2(\zeta_d)}{4\eta} [4 + 4A_1 \cos \theta_1 + A_1^2 + 4A_2 \cos \theta_2 + A_2^2 + 2A_1 A_2 \cos(\theta_1 - \theta_2)] \\ &= \frac{G^2(\zeta_d)}{4\eta} \left\{ 4 + \frac{4\rho_h DR_h G(\zeta_r)}{G(\zeta_d)} \cos(2\pi\delta/\lambda + \phi_h) + \frac{\rho_h^2 D^2 R_h^2 G^2(\zeta_r)}{G^2(\zeta_d)} \right. \\ &\quad \left. + \frac{4\rho_v DR_v G(\zeta_r)}{G(\zeta_d)} \cos(2\pi\delta/\lambda + \phi_v) + \frac{\rho_v^2 D^2 R_v^2 G^2(\zeta_r)}{G^2(\zeta_d)} + \frac{2\rho_h^2 D^2 R_h R_v G^2(\zeta_r)}{G^2(\zeta_d)} \cos(\phi_h - \phi_v) \right\} \end{aligned}$$

The power in the total transmitted wave is given above as:

$$S'_t = \frac{G^2(\zeta_d)}{2\eta} \left\{ 2 + \frac{2\rho_s DR_v G(\zeta_r)}{G(\zeta_d)} \cos(2\pi\delta/\lambda + \phi_v) + \frac{\rho_s^2 D^2 R_v^2 G^2(\zeta_r)}{G^2(\zeta_d)} \right. \\ \left. + \frac{2\rho_s DR_h G(\zeta_r)}{G(\zeta_d)} \cos(2\pi\delta/\lambda + \phi_h) + \frac{\rho_s^2 D^2 R_h^2 G^2(\zeta_r)}{G^2(\zeta_d)} \right\} \\ = \frac{G^2(\zeta_d) L_{multi}}{\eta}$$

where L_{multi} is the multipath loss defined as the ratio of total transmitted power to direct wave power. Polarization loss, which is the ratio of right-hand circular polarized power to total power is then given by

$$L_{pol} = \frac{S_r}{S'_t} = 1 - \frac{1}{4L_{multi}} \left[\frac{\rho_s^2 D^2 R_h^2 G^2(\zeta_r)}{G^2(\zeta_d)} + \frac{\rho_s^2 D^2 R_v^2 G^2(\zeta_r)}{G^2(\zeta_d)} - \frac{2\rho_s^2 D^2 R_h R_v G^2(\zeta_r)}{G^2(\zeta_d)} \cos(\phi_h - \phi_v) \right]$$

and this can be converted into dB by

$$L_{pol} (dB) = 10 \log_{10}(L_{pol})$$

All losses can be easily visualized by the vector diagram in Fig. 3. All vectors are normalized to $E_d = 1.0$ where E_d is the magnitude of the horizontal and vertical components of the circularly polarized direct wave. E_p is the magnitude of the wave at the peak of the antenna pattern. E_r is the magnitude of the reflected wave prior to reflection. Before any reflection from the planet's surface, E_p , E_d , and E_r are all in phase. After the reflected wave strikes the planet's surface, the horizontal and vertical components have magnitude and phase shift given

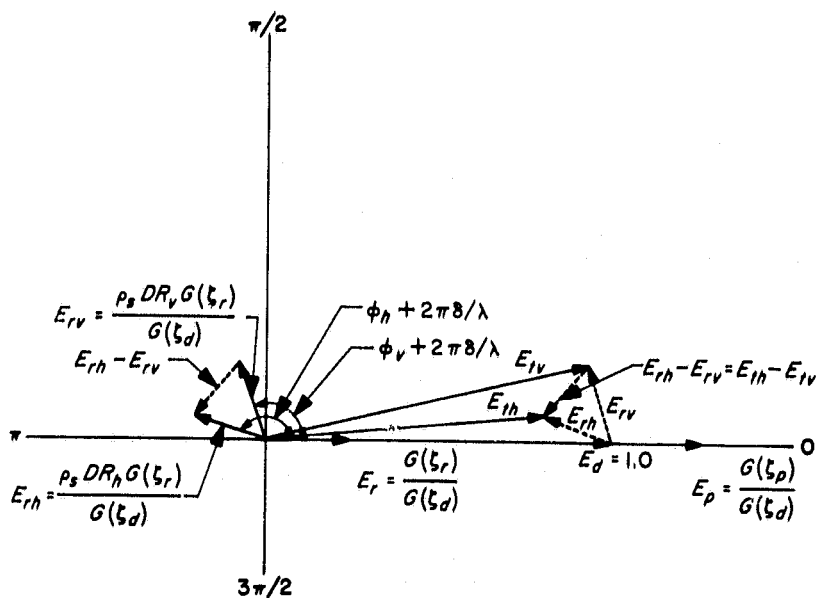


Fig. 3. CSAD lander radio electric field vector phase diagram

by E_{rh} and E_{rv} , respectively. These reflected fields are then vectorially added to E_d to get the horizontal and vertical components of the total wave given by E_{th} and E_{tv} , respectively. The angles ϕ_h and ϕ_v are also shown in the diagram.

The significance of the various losses is now readily apparent. Pointing loss is merely

$$L_{point} = \frac{|E_d|^2}{|E_p|^2} = \frac{1}{|E_p|^2}$$

Multipath loss is given by

$$L_{multi} = \frac{1}{2} (L_{multi}^- + L_{multi}^+) = \frac{1}{2} \left(\frac{|E_{th}|^2}{|E_d|^2} + \frac{|E_{tv}|^2}{|E_d|^2} \right) \\ = \frac{1}{2} (|E_{th}|^2 + |E_{tv}|^2)$$

Since

$$|E_{rh}| = \frac{\rho_s DR_h G(\zeta_r)}{G(\zeta_d)}$$

and

$$|E_{rv}| = \frac{\rho_s DR_v G(\zeta_r)}{G(\zeta_d)}$$

and since the angle between E_{rh} and E_{rv} is $\phi_h - \phi_v$, the polarization loss is seen to be

$$L_{pol} = 1 - \frac{\left| \frac{1}{2} (E_{rh} - E_{rv}) \right|^2}{\frac{1}{2} (|E_{th}|^2 + |E_{tv}|^2)} = 1 - \frac{\left| \frac{1}{2} (E_{th} - E_{tv}) \right|^2}{L_{multi}}$$

where the vectors are subtracted vectorially. The polarization loss is therefore seen to be unity minus the ratio of half the vectorial difference between the horizontal and vertical components squared to the multipath loss.

III. Coordinate Transformations

The lander communication link geometry is specified by giving the vector to earth receiver **E** and the vector to landing site **L** in Martian latitude and longitude, the direction and magnitude of slope **O** on which the lander rests, antenna boresight vectors **A**, and reflected wave vector **R**; therefore three coordinate systems are required to conveniently describe the direct link geometry: (1) a Mars-centered system in which to specify the earth and landing site vectors, (2) a landing-site-centered system in which to specify, (a) the direction and magnitude of the slope on which the lander rests, and (b) the transformed vector to earth, (3) a lander-centered system in which to specify the antenna boresight vectors and the transformed vector to earth.

For the sake of analytical convenience, the three coordinate systems will be assumed to have a common aerocentric origin, since the maximum parallax error would be on the order of the ratio of the Martian radius to the Mars-Earth distance.

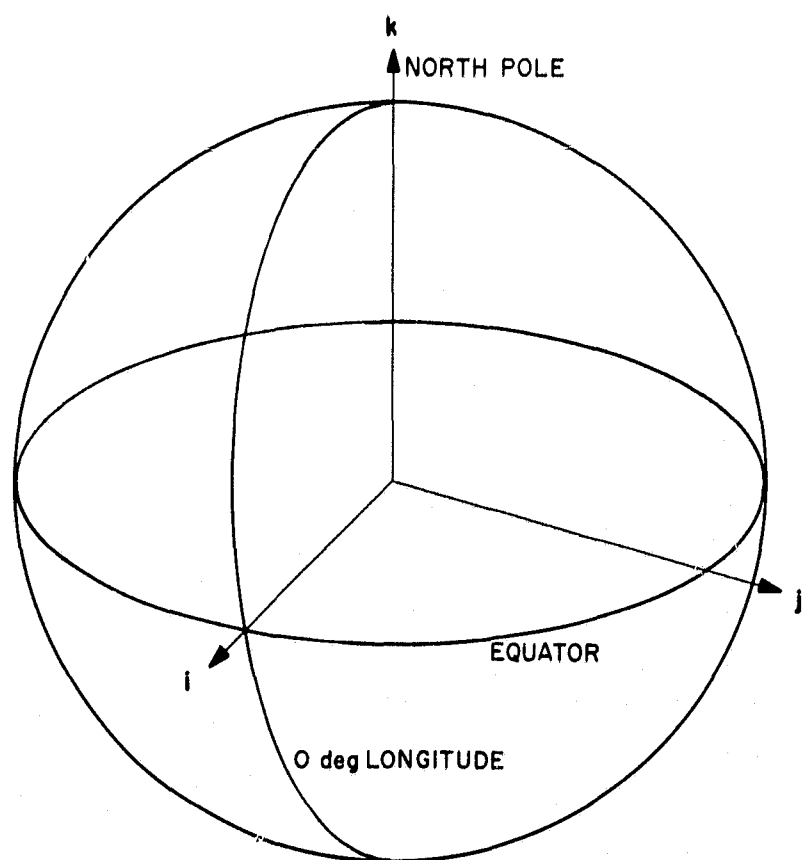


Fig. 4. Mars-centered coordinate system

In all coordinate systems, **i** vectors are the *x*-direction unit vectors, **j** vectors are the *y*-direction unit vectors, and **k** vectors are the *z*-direction unit vectors. Angles between a vector and the *x*-direction are designated by an α with an appropriate number of primes and a lower case subscript that is the same letter as the capitalized vector. Similarly, angles with respect to the *y* direction are designated β , and angles with respect to the *z* direction are designated γ , all with appropriate primes and subscripts. Quantities in the Mars-centered coordinate system are unprimed; quantities in the landing site-centered system are primed, and quantities in the lander-centered system are double-primed.

In the Mars-centered system, ϕ signifies latitude, and λ stands for longitude (both with appropriate subscripts); in the other two systems, θ (with appropriate primes and subscripts) is a cone angle measured from the *z* axis and ϕ , including its primes and subscripts, represents a clock angle, measured positively around the *z* axis from the *x* axis.

A. Mars-Centered Coordinate System

In the first (unprimed) coordinate system, shown in Fig. 4, **i** (the unit *x*-direction vector) is in the plane of the Martian equator through the 0 deg Martian longitude. The unit *y*-direction vector **j** is in the plane of the Martian equator through the 90 deg east longitude. The unit *z*-direction vector **k** is through the north Martian pole. The unprimed coordinate system is, therefore, based on Mars' latitude and longitude coordinates.

The vector **E** to the earth receiver can be written in terms of the latitude and longitude of the sub-earth point as

$$\mathbf{E} = \sin \phi_e \cos \lambda_e \mathbf{i} + \sin \phi_e \sin \lambda_e \mathbf{j} + \cos \phi_e \mathbf{k}$$

The direction cosines of **E** in terms of the sub-earth point latitude and longitude are then:

$$\cos \alpha_e = \sin \phi_e \cos \lambda_e$$

$$\cos \beta_e = \sin \phi_e \sin \lambda_e$$

$$\cos \gamma_e = \cos \phi_e$$

Similarly, the vector to the lander impact site can be given in terms of the landing site latitude and longitude:

$$\mathbf{L} = \sin \phi_l \cos \lambda_l \mathbf{i} + \sin \phi_l \sin \lambda_l \mathbf{j} + \cos \phi_l \mathbf{k}$$

The direction cosines of the impact site vector are then:

$$\cos \alpha_l = \sin \phi_l \cos \lambda_l$$

$$\cos \beta_l = \sin \phi_l \sin \lambda_l$$

$$\cos \gamma_l = \cos \phi_l$$

B. Landing-Site-Centered Coordinate System

In the second (primed) coordinate system, shown in Fig. 5, k' , the z' unit vector, points through the lander's position on the Martian surface and is, therefore, normal to the local horizontal and parallel to the impact site vector, L ; the x' unit vector i' is in the plane defined by k and k' , at right angles to k' , and pointing out through the northern hemisphere; j' , the y' unit vector, is in the

plane of the equator and 90 deg west of the longitude of i' and k' . The primed coordinate system is, therefore, based on the local horizontal coordinate system at the lander impact site.

The sub-earth vector can be transformed from the unprimed to the primed coordinate system by using the following transformation matrix:

	i	j	k
i'	$-\cos \phi_l \cos \lambda_l$	$-\cos \phi_l \sin \lambda_l$	$\sin \phi_l$
j'	$\sin \lambda_l$	$-\cos \lambda_l$	0
k'	$\sin \phi_l \cos \lambda_l$	$\sin \phi_l \sin \lambda_l$	$\cos \phi_l$

The direction cosines of E in the primed system are then:

$$\cos \alpha'_e = -\cos \phi_l \cos \lambda_l \cos \alpha_e - \cos \phi_l \sin \lambda_l \cos \beta_e + \sin \phi_l \cos \gamma_e$$

$$\cos \beta'_e = \sin \lambda_l \cos \alpha_e - \cos \lambda_l \cos \beta_e$$

$$\cos \gamma'_e = \sin \phi_l \cos \lambda_l \cos \alpha_e + \sin \phi_l \sin \lambda_l \cos \beta_e + \cos \phi_l \cos \gamma_e$$

The vector specifying the lander's orientation on the planet surface O can be written in terms of the lander's slope θ'_0 and the direction of slope (ϕ'_0). The direction cosines of O are:

$$\cos \alpha'_0 = \sin \theta'_0 \cos \phi'_0$$

$$\cos \beta'_0 = \sin \theta'_0 \sin \phi'_0$$

$$\cos \gamma'_0 = \cos \theta'_0$$

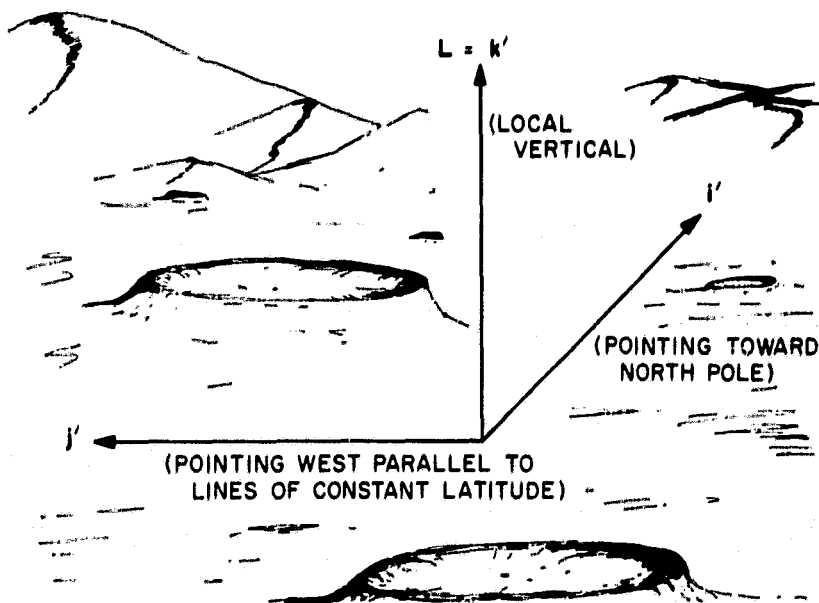


Fig. 5. Landing-site-centered coordinate system

C. Lander-Centered Coordinate System

In the third (double-primed) coordinate system, shown in Fig. 6, k'' , the z'' unit vector, is parallel to the lander

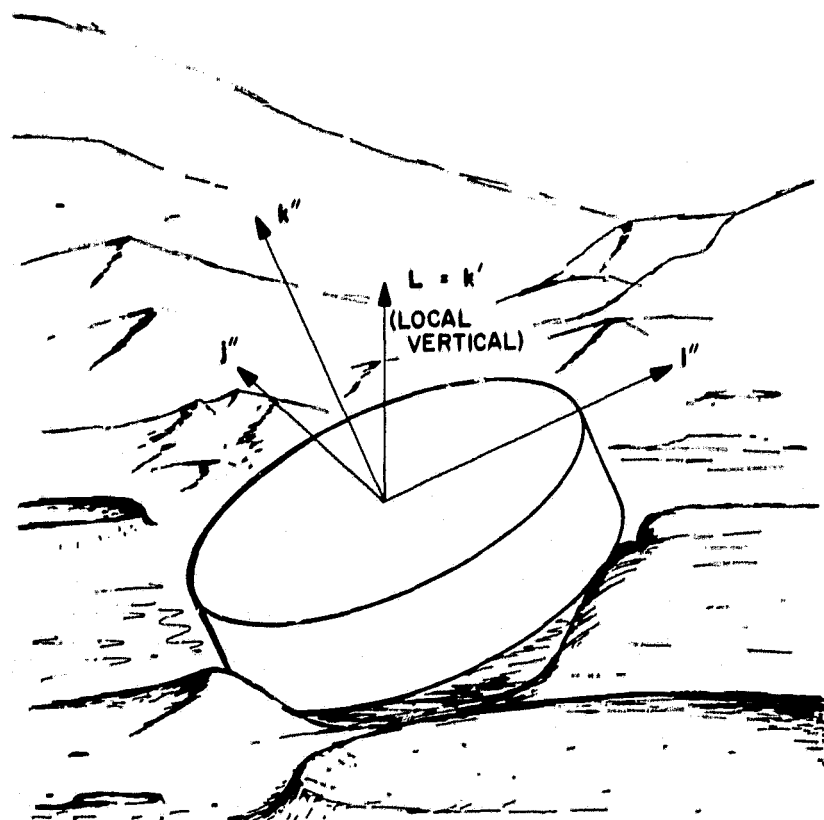


Fig. 6. Lander-centered coordinate system

roll axis and parallel to \mathbf{O} , the lander orientation vector. If we assume that the lander is resting on one of its flat sides and that the lander is parallel to the local slope, \mathbf{k}'' is then also normal to the local slope. The x'' unit vector, \mathbf{i}'' , is in the plane formed by \mathbf{k}'' and \mathbf{k}' , at right angles to \mathbf{k}'' , and at less than 90 deg angle from \mathbf{k}' . The unit y'' vector, \mathbf{j}'' , is in the $x''-y''$ plane and is the $\mathbf{k}'' \times \mathbf{i}''$ vector product. The double-primed coordinate system is, therefore, based on the lander's principal axes.

The sub-earth vector can be transformed from the primed to the double-primed system by using the follow-

ing transformation matrix:

	\mathbf{i}'	\mathbf{j}'	\mathbf{k}'
\mathbf{i}''	$-\cos \theta'_0 \cos \phi'_0$	$-\cos \theta'_0 \sin \phi'_0$	$\sin \theta'_0$
\mathbf{j}''	$\sin \phi'_0$	$-\cos \phi'_0$	0
\mathbf{k}''	$\sin \theta'_0 \cos \phi'_0$	$\sin \theta'_0 \sin \phi'_0$	$\cos \theta'_0$

The direction cosines of the sub-earth vector then become:

$$\cos \alpha'' = -\cos \theta'_0 \cos \phi'_0 \cos \alpha'_e - \cos \theta'_0 \sin \phi'_0 \cos \beta'_e + \sin \theta'_0 \cos \gamma'_e$$

$$\cos \beta'' = \sin \phi'_0 \cos \alpha'_e - \cos \phi'_0 \cos \beta'_e$$

$$\cos \gamma'' = \sin \theta'_0 \cos \phi'_0 \cos \alpha'_e + \sin \theta'_0 \sin \phi'_0 \cos \beta'_e + \cos \theta'_0 \cos \gamma'_e$$

The antenna boresight vector \mathbf{A} must also be specified by its direction cosines in the double-primed system in terms of its cone θ''_a and clock ϕ''_a angles. These relationships are

$$\cos \alpha''_a = \sin \theta''_a \cos \phi''_a$$

$$\cos \beta''_a = \sin \theta''_a \sin \phi''_a$$

$$\cos \gamma''_a = \cos \theta''_a$$

The direction of the reflected wave \mathbf{R} may similarly be specified in terms of its cone θ''_r and clock ϕ''_r angles. These relationships are

$$\cos \alpha''_r = \sin \theta''_r \cos \phi''_r$$

$$\cos \beta''_r = \sin \theta''_r \sin \phi''_r$$

$$\cos \gamma''_r = \cos \theta''_r$$

The cone and clock angles of \mathbf{R} can be determined by noting that the reflected wave must be in a plane containing both \mathbf{E} and \mathbf{O} and that its angle with the $x''-y''$ plane must be just the negative of the \mathbf{E} vector's angle with the $x''-y''$ plane; therefore

$$\theta''_r = \pi - \gamma''_e$$

$$\phi''_r = \phi''_e$$

The angular quantities required for computing losses can now be defined in terms of the lander-centered coor-

inate system. The grazing angle of the reflected wave (also the elevation of the earth above the local slope) is:

$$\gamma = \pi/2 - \gamma''_e$$

The angle between the antenna pattern maximum and the direction to earth is the scalar product of \mathbf{A} and \mathbf{E} ; therefore

$$\cos \zeta_a = \cos \alpha''_a \cos \alpha''_e + \cos \beta''_a \cos \beta''_e + \cos \gamma''_a \cos \gamma''_e$$

Similarly, the angle between the peak of the antenna pattern and the reflected wave direction is the scalar product of \mathbf{A} and \mathbf{R} ; thus:

$$\cos \zeta_r = \cos \alpha''_a \cos \alpha''_r + \cos \beta''_a \cos \beta''_r + \cos \gamma''_a \cos \gamma''_r$$

IV. Loss Results

For this specific case, it will be assumed that a lander of the CSAD class impacts Mars at 20 deg south latitude and 48 deg east longitude. It broadcasts immediately when the sub-earth point is at 17.6 deg south latitude and 0 deg longitude; it broadcasts again 21.3 h later when the sub-earth point is at 17.6 deg south latitude and 48 deg east longitude. These numbers are typical of a 1971 mission. Lander orientation will be computed probabilistically based on an assumed model of the Martian surface (see Appendix B). Antenna geometry will be that of a CSAD lander wherein six antennas are arrayed on the faces of an imaginary cube to assure omnidirectional coverage after impact. (See Table 1.) The

Table 1. Antenna configuration

Antenna No. <i>i</i>	1	2	3	4	5	6
h_i , cm	11.4	16.1	6.6	11.4	16.1	6.6
θ''_{a_i} , deg	90	45	135	90	45	135
ϕ''_{a_i} , deg	ϕ''_{a_i}	$\phi''_{a_i} + 90$	$\phi''_{a_i} + 90$	$\phi''_{a_i} + 180$	$\phi''_{a_i} + 270$	$\phi''_{a_i} + 270$

Note: ϕ''_{a_i} is a random variable with a uniform probability density function from 0 to 360 deg.

electrical quantities of the surface will be assumed similar to those of a dry earth soil and the wavelength will be that of the CSAD 2295 MHz S-band transmitter. The surface will be assumed to be flat in its large scale features and will have a 0.5 cm rms surface roughness. (See Appendix A for a justification of this assumption.) Antenna gain characteristics will be assumed to be those of the impactable CSAD cup radiator (see Appendix B).

The algebraic quantities associated with this case are then:

$$\text{Earth direction angles: } \begin{cases} \phi_e = 107.60 \text{ deg} \\ \lambda_e = 0 \text{ deg} \end{cases} \begin{cases} \text{immediately} \\ \text{after landing} \end{cases}$$

$$\begin{cases} \phi_e = 107.60 \text{ deg} \\ \lambda_e = 48 \text{ deg} \end{cases} \begin{cases} \\ \end{cases} \text{21.3 h later}$$

$$\text{Site direction angles: } \begin{cases} \phi_l = 110 \text{ deg} \\ \lambda_l = 48 \text{ deg} \end{cases}$$

Lander orientation angles: θ'_0 and ϕ'_0 derived from simulated landings on statistically modeled Martian surfaces.

Electrical quantities:

$$\epsilon/\epsilon_0 = 2$$

$$\mu/\mu_0 = 1$$

$$\sigma = 10^{-10} \text{ mho/cm}$$

$$\lambda = 13 \text{ cm}$$

Surface characteristics:

$$\Delta h = 0.5 \text{ cm}$$

$$D = 1$$

Antenna characteristics: From empirical gain plots of CSAD impactable antennas.

These quantities can then be used to compute the angles derived in Part III and the losses derived in Part II.

The distributions of losses of 100 computer-simulated landings immediately after landing and 100 landings 21.3 h after landing are given in Figs. 7 and 8. At each landing, pointing, multipath, polarization and combined losses are computed for each of the six antennas. The best (lowest) pointing, multipath, polarization, and combined loss is selected for each landing. These four best losses can conceivably occur on four different antennas, but the best combined loss usually occurs on the antenna with the best pointing loss. It will be noted that the best multipath loss is usually a gain rather than a loss, but this usually occurs on one of the antennas pointing away from the receiver so that the huge pointing loss overwhelms any multipath gain. It will also be noted that the best combined loss distribution closely follows the best pointing loss distribution since multipath and polarization losses are generally small for the antennas pointing toward the receiver. The mean combined loss with its 3σ tolerances can be expressed as $-2.2 \text{ dB} \pm_{2.5}^{2.4} \text{ dB}$ for the transmission immediately after landing and $-3.2 \text{ dB} \pm_{1.4}^{2.4} \text{ dB}$ for the transmission 21.3 h later when the earth is overhead.

V. Conclusions

Multipath, polarization, and pointing losses associated with a Mars lander communication link are shown to be much less severe than prior estimates which were based on the sum of worst case multipath, worst case polarization, and worst case pointing losses.

These losses were computed for the Jet Propulsion Laboratory (JPL) Capsule System Advanced Development (CSAD) Mars lander which is a disc-shaped rough lander. The lander obtained omnidirectional antenna coverage by having six antennas with their boresights perpendicular to the faces of an imaginary cube. The lander

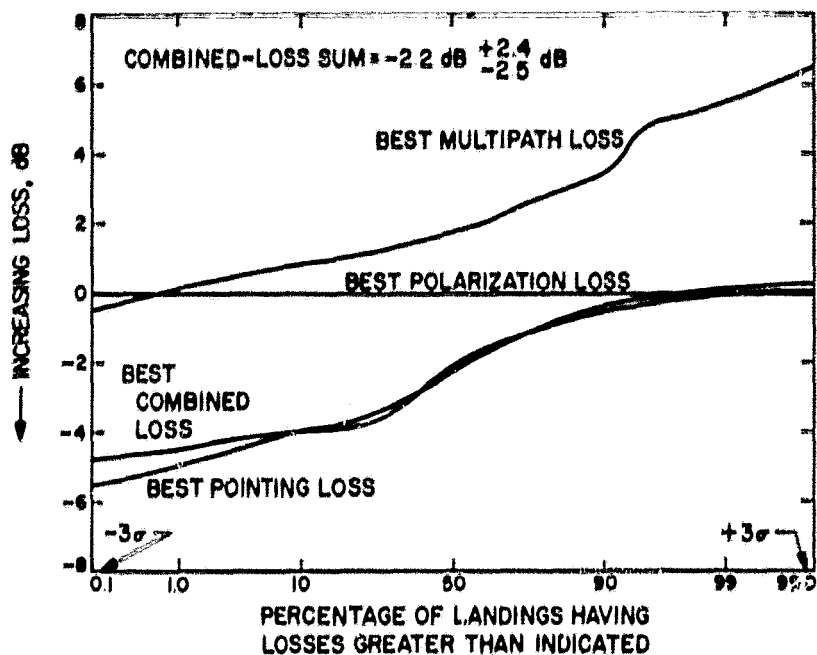


Fig. 7. Pointing, multipath, polarization, and combined loss distributions for circular polarization at landing

transmitted immediately upon landing when the earth was 45 deg above the western horizon and again the next day when the earth was overhead. The lander contained an S-band transmitter and six right-hand circularly polarized antennas.

The multipath, polarization, and pointing losses associated with the transmission immediately upon landing can be specified as $-2.2 \text{ dB} \pm_{2.5}^{2.4} \text{ dB}$. The losses associated with the transmission when the earth was overhead can be given as $-3.2 \text{ dB} \pm_{1.4}^{2.4} \text{ dB}$. These estimates are somewhat more realistic and more optimistic than prior worst-case predictions that might require excessively powerful and heavy radio and power subsystems and might reduce the scientific instrumentation payload.

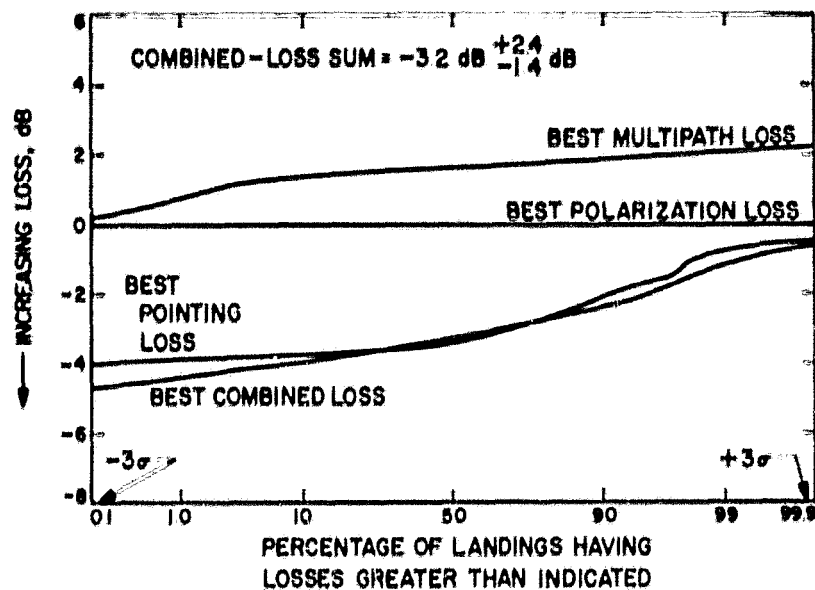


Fig. 8. Pointing, multipath, polarization, and combined loss distributions for circular polarization 21.3 h after landing

Several of the assumptions used in this analysis should be emphasized:

- (1) The reflected wave was assumed to be specularly reflected; diffuse reflection was neglected.
- (2) The planet's surface was assumed to be locally flat with a surface roughness reflection coefficient appropriate to a mean surface roughness of 0.5 cm.
- (3) The planet's electrical characteristics were assumed similar to dry earth: relative permeability = 1; relative dielectric constant = 2; and conductivity = 10^{-10} mho/cm.
- (4) The Martian surface was assumed to have an exponential distribution of surface slopes which closely approximates current surface slope estimates.

Reference

1. Beckmann, P., and Spizzichino, A., *The Scattering of Electromagnetic Waves from Rough Surfaces*, MacMillan Co., New York, 1963.

Appendix A

Computation of Fresnel Zones

In order for the assumption of specular reflection to be valid, the Rayleigh reflection criterion must be satisfied over the first Fresnel Zone. This criterion need be satisfied only over the first Fresnel Zone because the majority of the reflected energy comes from the first Fresnel Zone. This zone is an ellipse on the reflecting surface defined as the locus of points at which the reflected ray path lengths differ by $\lambda/2$ from the ray reflected at the optical reflection point. The path lengths of waves reflected from the second Fresnel Zone differ by λ from the optically reflected wave; the path lengths of waves from the third Fresnel Zone differ by $3\lambda/2$, etc. Since the waves from higher order Fresnel Zones differ in path lengths by $\lambda/2$, and since less energy is incident on and reflected from higher order Fresnel Zones, these waves tend to cancel

each other, leaving the waves reflected from the first Fresnel Zone as the dominant source of reflected energy. If the Rayleigh criterion is satisfied over this zone, specular reflection is a good assumption.

The Rayleigh criterion requires that $\Delta h < \lambda/8 \sin \gamma$ where Δh is the surface roughness, λ is the wavelength, and γ is the grazing angle. A curve defining the Rayleigh criterion for the 13 cm, S-band transmitter of the JPL CSAD program is shown in Fig. A-1.

Simple geometrical considerations show that the points on the first Fresnel ellipse closest to and farthest from a JPL CSAD lander antenna are given by the equation:

$$\frac{x^2}{\lambda^2} \sin^2 \gamma - \frac{x}{\lambda} \cos \gamma \left(1 + \frac{2h}{\lambda} \sin \gamma\right) + \frac{h^2}{\lambda^2} \cos^2 \gamma - \frac{h}{\lambda} \sin \gamma - \frac{1}{4} = 0$$

The roots of this quadratic are:

$$\frac{x}{\lambda} = \frac{\cos \gamma}{2 \sin^2 \gamma} + \left(\frac{h}{\lambda}\right) \frac{1}{\tan \gamma} \pm \left[\frac{1}{4 \sin^4 \gamma} + \left(\frac{h}{\lambda}\right) \frac{1}{\sin^3 \gamma} \right]^{1/2}$$

For the CSAD lander transmission at a noon landing

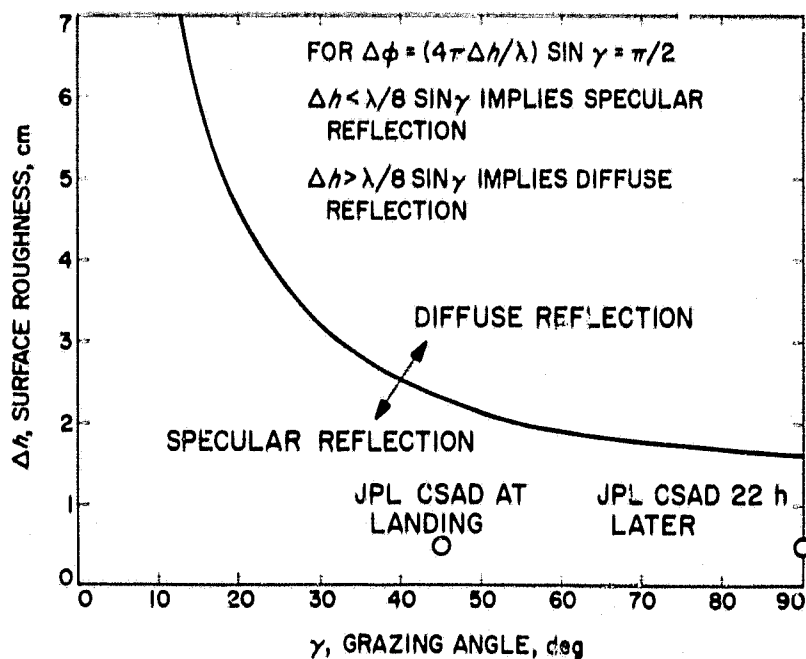


Fig. A-1. Rayleigh criterion for specular reflection at S-band (13 cm)

using one of the antennas in the plane of the lander, $h = 11.4$ cm, $\lambda = 13$ cm, and $\gamma = 45$ deg. The first Fresnel ellipse extends from 3.5 cm behind the antenna to 44.7 cm in front of it. For a CSAD lander transmission with the earth overhead, the first Fresnel ellipse degenerates to a 13.6 cm radius circle. The Rayleigh criterion is very likely satisfied over these relatively small areas so that specular reflection is a good assumption. The Fresnel Zone calculation geometry is shown in Fig. A-2.

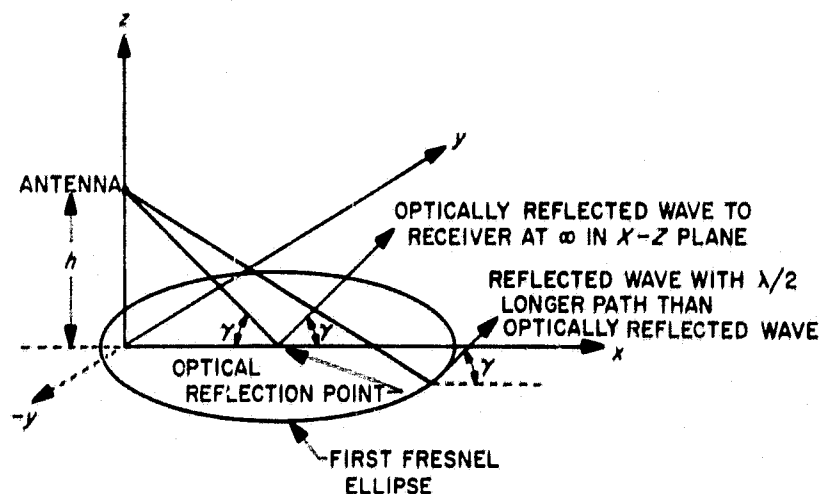


Fig. A-2. Fresnel zone calculation geometry

Appendix B

Random Variable Distributions and Antenna Characteristics

This computer simulation of Mars lander losses requires three random variables: (1) the slope on which the lander impacts (θ'_0); (2) the direction of the slope on which the lander impacts (ϕ'_0); and (3) the clock angle of the lander antenna boresight (ϕ''_a).

The slope probability density function is shown in Fig. B-1. Estimated probability density functions of Martian slopes in both mountainous and level areas are compared with the approximate exponential distribution used in the computer simulation.

The computer generates the slope by first picking one of the 10^4 random numbers between 0000 and 9999. This random number is then divided by 10^4 to obtain one of 10^4 random fractions between 0.0000 and 0.9999. If the

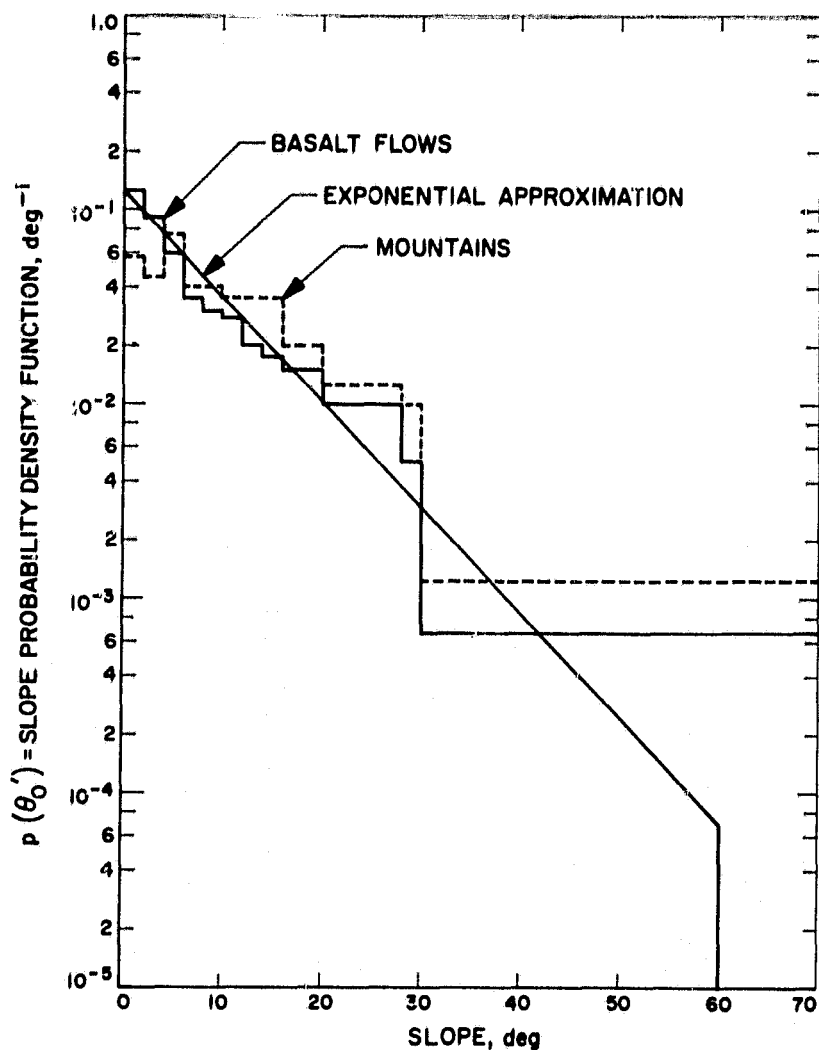


Fig. B-1. Probability density functions of Martian slopes

probability density function, $q(x)$, of these random numbers, x , is then represented by a uniform, continuous $q(x) = 1$ for $0 \leq x \leq 1$, and if the exponential approximation of the Martian slope probability density function is given by $p(\theta'_0) = \lambda \exp - \lambda \theta'_0$, we can determine a functional relationship between x and θ'_0 such that the uniformly distributed random variable x generates θ'_0 according to the assumed probability density function of θ'_0 . We are looking for a function, $\theta'_0 = f(x)$ that has a probability density function $p(\theta'_0)$ if x 's probability density function is $q(x) = 1$. Equating differential probabilities of the two variables:

$$-p(\theta'_0) d\theta'_0 = q(x) dx$$

Dividing by $q(x) d\theta'_0$:

$$\frac{dx}{d\theta'_0} = -\frac{p(\theta'_0)}{q(x)} = -\lambda \exp - \lambda \theta'_0$$

Integrating:

$$x = \exp - \lambda \theta'_0$$

Inverting:

$$\theta'_0 = \frac{-1}{\lambda} \ln(x)$$

which is the relationship used to generate θ'_0 from the uniformly distributed random fraction x . The approximation shown in Fig. B-1 used $\lambda = 0.125$.

The random direction of the slope on which the lander hits and the random clock angle of the antenna boresight vector are just uniformly distributed angles between 0 and 360 deg; therefore if x is again the uniformly distributed random fraction between 0 and 1, the function used to generate ϕ'_0 and ϕ''_a is simply: $\phi'_0 = \phi''_a = 360x$.

A rectangular cup antenna, similar to one of the JPL CSAD lander antennas, was used as the antenna model. Gain curves in two orthogonal directions are shown in Fig. B-2 for this antenna. Also plotted in that figure is the eighth degree polynomial approximation used in the computer to generate the antenna gain curve.

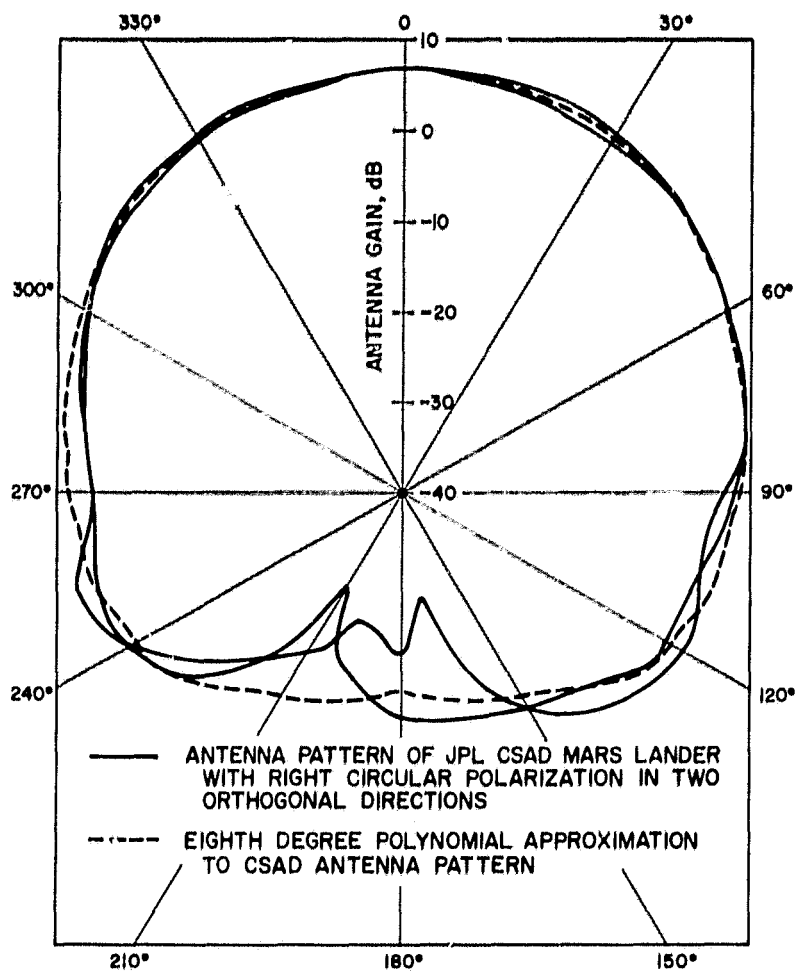


Fig. B-2. Antenna gain characteristics

Appendix C

Losses as a Function of Mars Rotation

Multipath, pointing, and combined multipath and pointing losses were computed for a fixed lander orientation as a function of planet rotation in order to determine whether sudden nulls would occur in the signal received on earth. It was determined that the combined losses varied only slightly as a function of Mars rotation. The comparatively small polarization losses were neglected for the purposes of this check for sudden nulls.

In this analysis, the lander was assumed to land on a flat surface with antenna number one pointing north. The landing was assumed to take place at approximately noon

when the earth was 45 deg above the western horizon. Multipath, pointing, and combined losses were computed from about 40 min before a nominal landing until 40 min after a nominal landing. Losses were computed every 24 s during this 80-min period. Combined losses as a function of planet rotation are plotted for each antenna in Fig. C-1. In the particular orientation chosen, antenna 5 points almost directly at earth; antennas 1, 2, 4, and 6 point about 90 deg from the earth direction, and antenna 3 points directly away from the earth. In no case do the combined losses vary rapidly over the 80-min period considered.

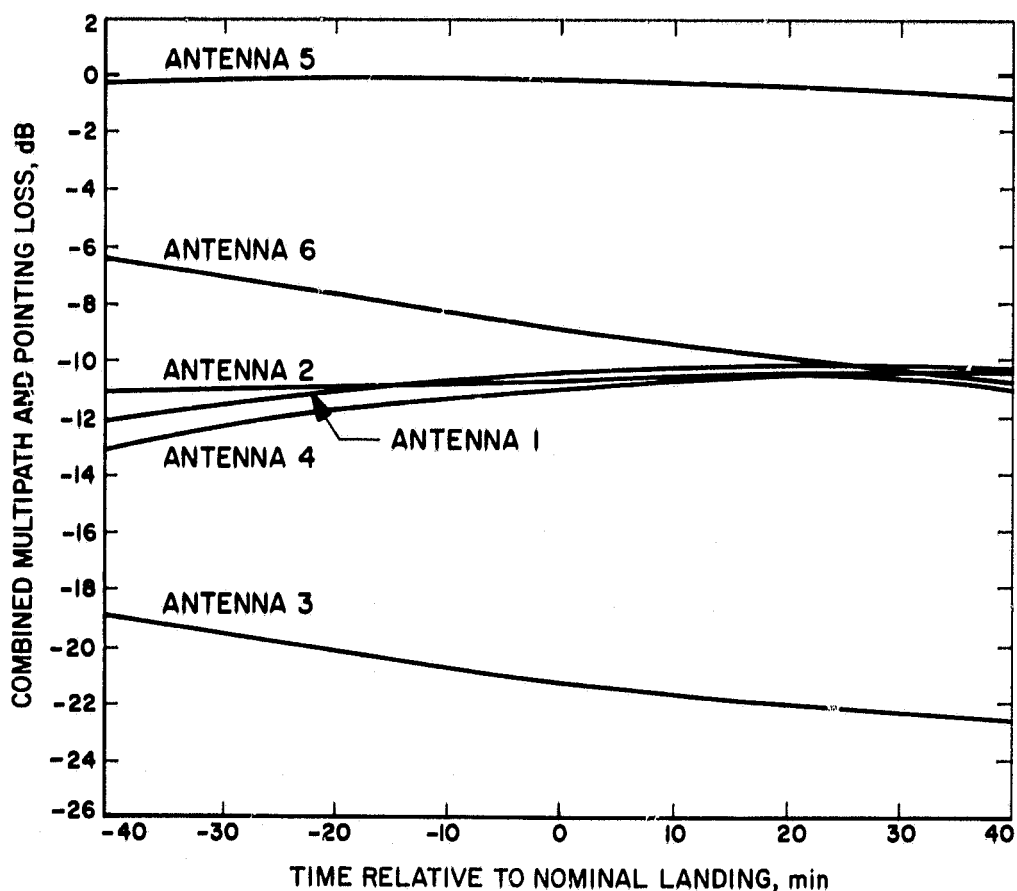


Fig. C-1. Multipath and pointing losses vs planet rotation

Appendix D

Computer Program for Loss Computation

```

C AD6 L. A. HOWARD
C MULTIPATH DEGRADATION AND POINTING LOSS FOR ANTENNA
C ALSO POLARIZATION LOSS - AD6 ONLY
C AD1 FOR VERTICAL POLARIZATION
C AD2 FOR HORIZONTAL POLARIZATION
C AD3=AD1 FOR BEST ANTENNA PER LANDING
C AD4=AD2 FOR BEST ANTENNA PER LANDING
C AD5 FOR RIGHT HAND CIRCULAR POLARIZATION (FORMAT AS PER AD3)
C AD6 SIMILAR TO AD5 BUT INCLUDES POLARIZATION LOSS IN ADDITION
C TOT MUST NOT EXCEED 100
  DIMENSION ARM(16),ARP(16),ARMS(16),ARPS(16),GA(9),
  IAM(100),AP(100),AS(100),ASMS(16),ASUM(16),APOLA(100),APPS(16),
  ZAPP(16)
  COMMON ABD
  NNN=1
  DO 17 I=1,100
  AM(I)=-50.
  AP(I)=-50.
  APOLA(I)=-50.
17 AS(I)=-50.
  ASM=0.
  AVM=0.
  AVP=0.
  DO 5 JJ=1,16
  ARM(JJ)=0.
  APP(JJ)=0.
  ASUM(JJ)=0.
  5 ARP(JJ)=0.
  DR=1.74532925E-02
  RD=57.3
  PI=3.1415927
  READ 50,TOT,W1,W2,W3,W4,W5,W6
  READ 10,THL,PHL
  READ 20,EPS,EPSD,AMU,AMUD,ALMDA,SIG,GZERO
  READ 30,(GA(I),I=1,9)
  1 CONTINUE
  READ 40,ABD,THE,PHE,THAPP,DD,H,DH,PPADD,ANUMB
  10 FORMAT (2F8.3)
  20 FORMAT (7F10.5)
  30 FORMAT (3E16.8)
  40 FORMAT (8F8.3,F8.0)
  50 FORMAT (F8.3,6A4)
  NTOT=TOT
  THER=THE*DR
  PHER=PHE*DR
  THLR=THL*DR
  PHLR=PHL*DR
  TAPPR=THAPP*DR
  NUMB=ANUMB
  DO 350 J=1,NTOT
2001 CALL RANDOM (I3)
  AB=IB
  AB=AB/10000.
  THOP=-8.*LOG(AB)
  IF (THOP-60.)2002,2002,2001
2002 CONTINUE
  CALL RANDOM (IB)
  AB=IB
  PHAPP=360.*AB/10000.+PPADD

```

```

CALL RANDOM (IB)
AB=IB
PHOP=360.*AB/10000.
TOPR=THOP*DR
POPR=PHOP*DR
PAPPR=PHAPP*DR
CAE=SIN(THER)*COS(PHER)
CBE=SIN(THER)*SIN(PHER)
CGE=COS(THER)
GEP=SIN(THLR)*COS(PHLR)*CAE+SIN(THLR)*SIN(PHLR)*CBE+COS(THLR)*CGE
BEP=SIN(PHLR)*CAE-COS(PHLR)*CBE
AEP=-COS(THLR)*COS(PHLR)*CAE-COS(THLR)*SIN(PHLR)*CBE+SIN(THLR)*CGE
GEPP=SIN(TOPR)*COS(POPR)*AEP+SIN(TOPR)*SIN(POPR)*BEP+COS(TOPR)*GEP
BEPP=SIN(POPR)*AEP-COS(POPR)*BEP
A2P=-COS(TOPR)*COS(POPR)*AEP-COS(TOPR)*SIN(POPR)*BEP+SIN(TOPR)*GEP
AEPP=A2P
GAPP=COS(TAPPR)
BAPP=SIN(TAPPR)*SIN(PAPPR)
AAPP=SIN(TAPPR)*COS(PAPPR)
ABC=GEPP**2
BCD=1.-ABC
BCD=SQRT(BCD)
RGEPP=ATAN(BCD/GEPP)
IF (RGEPP) 150, 160, 160
150 RGEPP=RGEPP+PI
160 CONTINUE
GAM=PI/2.-RGEPP
IF (GAM) 1001, 1002, 1002
1002 CONTINUE
CZED=AAPP*AEPP+BAPP*BEPP+GAPP*GEPP
CZER=AAPP*AEPP+BAPP*BEPP-GAPP*GEPP
DEL=(H/SIN(GAM))*(1.-COS(2.*GAM))
ANU=-60.*ALMDA*SIG*AMUO/AMU
TH1=ATAN(ANU/((EPS*AMUO/(EPSO*AMU))-COS(GAM)**2))
TH1=TH1/2.
A1=((EPS*AMUO/(EPSO*AMU))-COS(GAM)**2)**2+ANU**2)**0.25
Y2=ANU*SIN(GAM)+A1*SIN(TH1)
Y1=ANU*SIN(GAM)-A1*SIN(TH1)
X2=EPS*AMUO*SIN(GAM)/(EPSO*AMU)+A1*COS(TH1)
X1=EPS*AMUO*SIN(GAM)/(EPSO*AMU)-A1*COS(TH1)
Y3=(X2*Y1-X1*Y2)/(X2**2+Y2**2)
X3=(X1*X2+Y1*Y2)/(X2**2+Y2**2)
RHOS=EXP(-0.5*(4.*PI*DH*SIN(GAM)/ALMDA)**2)
IF (X3) 134, 131, 131
131 TH2=ATAN(Y3/X3)+2.*PI*DEL/ALMDA
GO TO 138
134 TH2=ATAN(Y3/X3)+PI+2.*PI*DEL/ALMDA
138 CONTINUE
ABC=CZED**2
BCD=1.-ABC
BCD=SQRT(BCD)
ZED=ATAN(BCD/CZED)
IF (ZED) 165, 170, 170
165 ZED=ZED+PI
170 CONTINUE
ABC=CZER**2
BCD=1.-ABC
BCD=SQRT(BCD)
ZER=ATAN(BCD/CZER)

```

```

      IF (ZER)175,180,180
175  ZER=ZER+PI
180  CONTINUE
      D=ZED*RD
      R=ZER*RD
      GD=GA(1)+D*(GA(2)+D*(GA(3)+D*(GA(4)+D*(GA(5)+D*(GA(6)+D*(GA(7)+
1D*(GA(8)+D*(GA(9))))))))
      GR=GA(1)+R*(GA(2)+R*(GA(3)+R*(GA(4)+R*(GA(5)+R*(GA(6)+R*(GA(7)+
1R*(GA(8)+R*(GA(9))))))))
      GD=EXP(2.3025851*GD/20.)
      GR=EXP(2.3025851*GR/20.)
      GM=EXP(2.3025851*GZERO/20.)
      A2=GR*(X3**2+Y3**2)**0.5*DD*RHOS
      A3=SQRT((GD+A2*COS(TH2))**2+A2**2*SIN(TH2)**2)
      Y4=-A1*SIN(TH1)
      X5=SIN(GAM)+A1*COS(TH1)
      X4=SIN(GAM)-A1*COS(TH1)
      Y6=(X4*Y4+X5*Y4)/(X5**2+Y4**2)
      X6=(X4*X5-Y4**2)/(X5**2+Y4**2)
      IF (X6)1134,1131,1131
1131 TH4=ATAN(Y6/X6)+2.*PI*DEL/ALPHA
      GO TO 1138
1134 TH4=ATAN(Y6/X6)+2.*PI*DEL/ALPHA+PI
1138 CONTINUE
      A4=GR*DD*RHOS*(X6**2+Y6**2)**0.5
      A5=SQRT((GD+A4*COS(TH4))**2+A4**2*SIN(TH4)**2)
      AMULTI=10.*0.43429448*LOG((A3**2+A5**2)/(2.*GD**2))
      APOINT=20.*0.43429448*LOG(GD/GM)
      POLA=(A2/GD)**2+(A4/GD)**2
      POLB=2.*A2*A4*COS(TH2-TH4)/GD**2
      POLC=4.*(A3**2+A5**2)/(2.*GD**2)
      APOL=10.*0.43429448*LOG(1.-(POLA-POLB)/POLC)
      GO TO 1999
1001 AMULTI=-50.
      APOINT=-50.
      APOL=-50.
1999 CONTINUE
      ASMP=AMULTI+APOINT+APOL
      PRINT 1000,NNN,J,AMULTI,APOINT,APOL,ASMP
1000 FORMAT (1X4HANT.,1X11,2X5HLAND.,1X14,5X5HMULTI,F8.3,2X5HPPOINT,F8.3
1,2X3HPOL,F8.3,2X3HSUM,F8.3)
      IF (AMULTI-AM(J))310,310,300
300 AM(J)=AMULTI
310 IF (APOINT-AP(J))320,320,315
315 AP(J)=APOINT
320 IF (ASMP-AS(J))322,322,321
321 AS(J)=ASMP
322 IF (APOL-APOLA(J))350,350,349
349 APOLA(J)=APOL
350 CONTINUE
      NNN=NNN+1
      PRINT 3000
      IF (NNN-7)1,376,376
376 DO 380 J=1,NTOT
      AVM=AVM+AM(J)
380 ASM=ASM+AS(J)
      DO 1050 JJJ=1,NTOT
1050 PRINT 2000,JJJ,AM(JJJ),AP(JJJ),APOLA(JJJ),AS(JJJ)
2000 FORMAT (1X4HBEST,2X4HLAND,I4,4X5HMULTI,F8.3,2X5HPPOINT,F8.3,2X3HPOL

```

```

1,F8.3,2X3HSUM,F8.3)
PRINT 3000
ASM=ASM/TOT
AVM=AVM/TOT
DO 375 JJ=1,16
AJ=JJ
ARMS(JJ)=AVM-7.5+(AJ-1.)
ARPS(JJ)=-7.5+(AJ-1.)*0.5
APPS(JJ)=-0.03+(AJ-1.)*0.002
ASMS(JJ)=ASM-7.5+(AJ-1.)
375 CONTINUE
DO 500 J=1,NTOT
400 DO 500 JJ=1,16
IF (AM(J)-ARMS(JJ))405,410,410
405 ARM(JJ)=ARM(JJ)+1.
410 IF (AP(J)-ARPS(JJ))415,420,420
415 ARP(JJ)=ARP(JJ)+1.
420 IF (AS(J)-ASMS(JJ))425,498,498
425 ASUM(JJ)=ASUM(JJ)+1.
498 IF (APOLA(J)-APPS(JJ))499,500,500
499 APP(JJ)=APP(JJ)+1.
500 CONTINUE
PRINT 721
721 FORMAT (1H ,36X5HRHCP ,////////)
PRINT 600
600 FORMAT (1H ,29X15HANTENNA (BEST) ,//2X9HMULTIPATH,23X8HPOINTING,23
1X12HPOLARIZATION,/1X11HDEGRADATION,4X8HQUNANTITY,12X4HLOSS,6X8HQUN
2TITY,15X4HLOSS,6X8HQUNANTITY,/5X4H(DB),6X10HLESS THAN,11X4H(DB),
35X10HLESS THAN,14X4H(DB),5X10HLESS THAN,15X11HSUM RESULTS,/)
DO 610 I=1,16
610 PRINT 625,ARMS(I),ARM(I),ARPS(I),ARP(I),APPS(I),APP(I),ASMS(I),
1ASUM(I)
625 FORMAT (3XF8.3,7XF6.0,11XF8.3,3XF6.0,13XF8.3,5XF6.0,13XF8.3,5XF6.0
1)
PRINT 650,NTOT
650 FORMAT (//,27X17HNUMBER OF SAMPLES,2XI4)
PRINT 750,W1,W2,W3,W4,W5,W6
750 FORMAT (////////,26X6A4)
3000 FORMAT (1H1)
900 CALL EXIT
END

```